Hindawi
Advances in Civil Engineering
Volume 2019, Article ID 4079217, 18 pages
https://doi.org/10.1155/2019/4079217

Research Article

Design Earthquake Response Spectrum Affected by Shallow Soil Deposit

Dong-Kwan Kim,[1] **Hong-Gun Park**,[2] **and Chang-Guk Sun**[3]

[1]*Department of Architectural Engineering, Cheongju University, Cheongju 28503, Republic of Korea*
[2]*Department of Architectural and Architectural Engineering, Seoul National University, Seoul 08826, Republic of Korea*
[3]*Earthquake Research Centre, Korea Institute of Geoscience and Mineral Resources, Daejeon 34132, Republic of Korea*

Correspondence should be addressed to Dong-Kwan Kim; dkkim17@cju.ac.kr

Received 23 October 2018; Revised 2 February 2019; Accepted 19 February 2019; Published 19 March 2019

Academic Editor: Jorge Branco

Site response analyses were performed to investigate the earthquake response of structures with shallow soil depth conditions in Korea. The analysis parameters included the properties of soft soil deposits at 487 sites, input earthquake accelerations, and peak ground-acceleration levels. The response spectra resulting from numerical analyses were compared with the design response spectra (DRS) specified in the 2015 International Building Code. The results showed that the earthquake motion of shallow soft soil was significantly different from that of deep soft soil, which was the basis of the IBC DRS. The responses of the structures were amplified when their dynamic periods were close to those of the site. In the case of sites with dynamic periods less than 0.4 s, the spectral accelerations of short-period structures were greater than those of the DRS corresponding to the site class specified in IBC 2015. On the basis of these results, a new form of DRS and soil factors are proposed.

1. Introduction

The 1985 Mexico City earthquake clearly showed that the earthquake responses of buildings can be significantly amplified by soft subsoils. Thus, in current design codes, site coefficients are used to address the effects of the subsoil. In the Korean Building Code 2016 [1], the design response spectrum (DRS) and the site coefficients are similar to those in the International Building Code 2015 [2]. The site coefficients in IBC 2015 were based on earthquake ground motions measured at sites located on the West Coast of the United States that have deep soil depths (depth to bedrock = 150–300 m) [3]. The site class in IBC 2015 is specified by the average shear-wave velocity, $V_{S,30}$, of the top 30 m of soil.

In Korea, however, the soil depth to the bedrock is relatively shallow, ranging from 6 to 100 m (mostly < 30 m). Thus, in most cases, the properties of the entire soil depth can be investigated. More importantly, the shallow soil depth significantly affects the responses of structures. Previous studies and other design codes [4, 5] have shown that the dynamic periods of the soil vary significantly with soil depth, even for the same soil shear-wave velocity (i.e., shear stiffness). This result indicates that the response spectrum and site coefficients for the earthquake design of structures should be defined by the dynamic period of the subsoil, which includes the effects of the soil depth as well as the soil material properties.

In EUROCODE-8 [6], recognizing the effect of shallow soil depth, when the soil depth to bedrock is less than 20 m and the property of the stiff bedrock is included in the estimation of $V_{S,30}$, the site class is categorized as a special soil class, S_E. The New York City Department of Transportation [7] developed a new DRS for their metro area, considering the effect of the shallow soil depth in the region. The Mid-America Earthquake Center (MAE) proposed uniform hazard ground motions and response spectra for mid-American cities that are located in regions with moderate seismicity. Hwang et al. [8] proposed site coefficients for the Eastern United States with shallow soil

depths. In Korea, Kim and Yoon [9] proposed a new site classification and new site coefficients for regions with shallow soil depths.

In the present study, site response numerical analyses were performed using an equivalent linear analysis method for 487 sites in Korea, considering the local geological and dynamic site properties. In total, 18 earthquake motions with three acceleration levels were used as the input for the numerical analysis. Based on the analyses, a new form of DRS and site classification were developed to describe the effects of shallow soil depth on the responses of structures. For this purpose, the following three steps were studied. In the first step, maintaining the definitions of the site factors in IBC 2015, the values of the site factors were modified on the basis of the numerical analyses for shallow soil depths. The resulting response spectrum is denoted as DRS-1. In the second step, the site class was defined by the site period and amplification factors, F_a and F_v, were defined as a function of the site period (DRS-2). In the third step, the shape of the DRS and the site coefficients were modified considering the effect of the site period (DRS-3).

2. Numerical Analyses of Site Response

2.1. Site Conditions. In the present study, 487 sites in Korea were considered. Among them, the properties of 378 sites in Figure 1 were obtained from the geotechnical information system (GTIS), developed by Sun et al. [10]. Using existing data from boring tests and topographical surveys, the GTIS with 100×100 m grids was developed for the Seoul city area (39.0×34.0 km). From the GTIS, the thicknesses of four soil/rock strata (fill soil, alluvial soil, weathered soil, and weathered rock) above the bedrock were obtained. The representative shear-wave velocities of the fill soil, alluvial soil, weathered soil, and weathered rock were determined as 190, 280, 350, and 650 m/s, respectively, based on the statics of the shear-wave velocity profiles measured at the sites. Additionally, in Figure 2, 109 shear-wave velocity profiles previously reported by Lee et al. [11] were used for site conditions.

Table 1 summarizes the soil properties of the 487 sites. According to the site classification $V_{S,30}$ [2], the soil properties are classified as S_B, S_C, S_D, and S_E, corresponding to 9, 302, 161, and 15 sites, respectively. At the S_B sites, the maximum depth to bedrock was 10 m; the site periods range from 0.047 s to 0.075 s when an elastic soil property is assumed. At the S_C sites, the depth to bedrock and the site periods range from 5.3 to 91.6 m and from 0.058 to 0.66 s, respectively. At the S_D sites, the depth to bedrock ranges from 12.2 to 84.1 m, which is close to that of the S_C sites. However, the site period at the S_D sites was in the range of 0.24 to 0.96 s, which is greater than that of the S_C sites. At the S_E sites, the site periods were much greater, even for extremely shallow soil depths. These results indicate that even for the same site class, the site period vary significantly and both the shear-wave velocities and the soil depth to bedrock should be considered to accurately define the dynamic properties of the site. Figure 3 clearly shows the relationship between the soil depth and the site period. Even for the same site class, the site period increased in proportion to the soil depth. Thus, the dynamic properties of the soil should be defined by the site period because the acceleration of structures is amplified by resonance with a subsoil having a similar period. The dynamic period of the sites can be calculated by the first-mode frequency, f_1, of the wave-propagation transfer function. When the soil is subjected to a large inelastic deformation, the soil stiffness decreases. Thus, the actual soil period is greater than the elastic soil period. To consider the nonlinear properties of the soil and rock in Figure 4, the effective shear modulus proposed by Kim and Choo [12] was used for an equivalent linear analysis of the subsoil.

2.2. Input Accelerations. For the one-dimensional equivalent linear analysis [13], 12 actual earthquake accelerations and 6 artificial accelerations were used for the input. The 12 actual accelerations, recorded at rock sites, were selected from the PEER Ground Motion Database [14]. Table 2 shows the properties of the actual earthquake accelerations: the magnitude, the mechanism, and the distance. In the Korean Building Code [1], the reference effective ground accelerations for the 500-, 1,000-, and 2,400-year return periods were defined as 0.11 g, 0.154 g, and 0.22 g, respectively. The existing earthquake-acceleration records were scaled to the reference effective ground-acceleration levels, as follows. First, a response spectrum was calculated from the time-history analysis of the existing records, assuming the S_B site class. By comparing the response spectrum with the DRS of the KBC (same as the spectrum in IBC 2015), the scale factor for each earthquake record was determined. The scaling factor α in equation (1) was determined such that the difference, D_s, in equation (2) (between the response spectrum of the earthquake accelerations and the DRS) was minimized using the condition of $d(D_s)/d\alpha = 0$ [15]:

$$\alpha = \frac{\sum_{T=T_a}^{T_b} \left(S_a^R(T) S_a^T(T)\right)}{\sum_{T=T_a}^{T_b} \left(S_a^R(T)\right)^2}, \tag{1}$$

$$D_s = \int_{T_a}^{T_b} \left[\alpha S_a^R(T) - S_a^T(T)\right]^2 dT, \tag{2}$$

where S_a^R and S_a^T are the response spectral accelerations obtained from the earthquake records and the design code, respectively, T is the period of the structure, and T_a and T_b are the lower and upper periods for the scaling. In this study, T_a and T_b were assumed as 0.1 s and 1.5 s, respectively, for the DRS of S_B [16]. In this study, the constant scale factors for the reference effective ground accelerations were calculated and used. Because the constant scale factor might cause large differences for particular period ranges, the scaled accelerations with the large differences were not used. Figure 5 shows time histories and response spectra of selected 12 actual accelerations.

The artificial earthquake accelerations were generated according to Gasparini and Vanmarche [17]. The envelope of the acceleration time history that controls the superposition of the harmonic functions was assumed as a

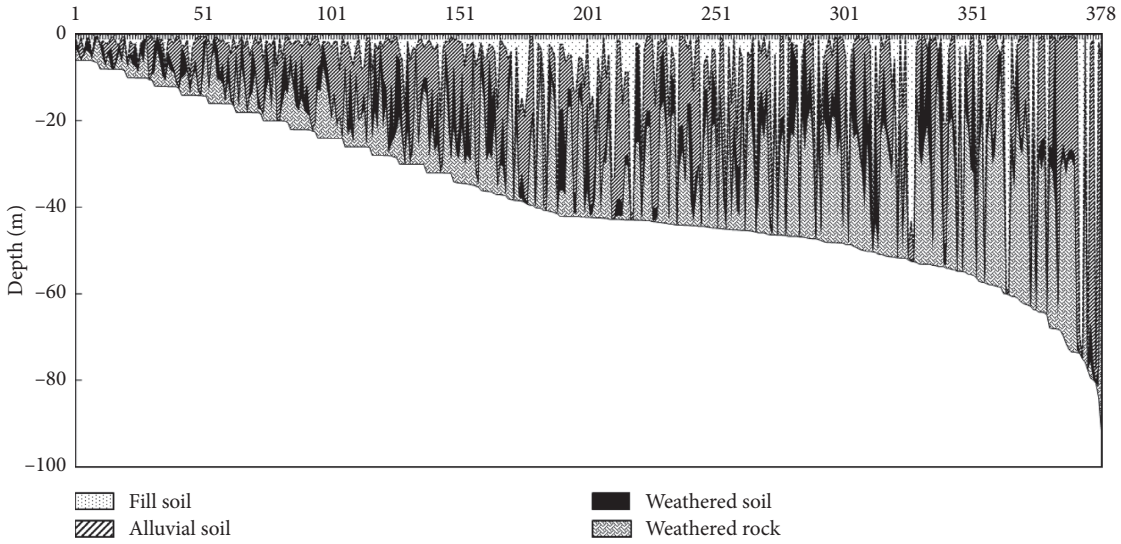

Figure 1: 378 soil strata from GTIS.

trapezoidal function. The starting time and duration of the acceleration time history were defined as T_{rise} and T_{level}, respectively. In the ASCE standard 4-98 [18], 1.5 s and 10 s were recommended for T_{rise} and T_{level}, respectively, for regions that have an expected maximum earthquake magnitude of 6.5–7.0. However, the Ministry of Construction and Transportation in Korea [19] recommended 2 s and 6–7 s for T_{rise} and T_{level}, respectively, based on the earthquake accelerations measured in Korea. In the present study, six artificial earthquakes were generated using 1.5 s and 2.5 s for T_{rise} and 6.0 s, 8.0 s, and 10.0 s for T_{level}. Figure 6 compares the DRS of the KBC (site class S_B), the response spectra from the scaled-input accelerations, and the average response spectrum. The average response spectrum was close to the DRS, indicating that the scaling method was acceptable.

3. Parametric Study and Results

3.1. Results for All 487 Sites. Figure 7 shows the numerical analysis results for 487 sites in the case of reference effective peak ground acceleration (EPGA) = 0.22 g. In the figure, each response spectrum indicates the average of the results calculated from 18 input accelerations (i.e., the number of actual response spectra is 18 times the results shown in the figure). The results were classified by the site-class criteria $V_{S,30}$ of IBC 2015. For the S_B to S_D sites (Figures 7(a)–7(c)), the maximum spectral accelerations of the short-period structures were significantly greater than the DRS values of IBC 2015. For the S_E sites, on the other hand, the spectral accelerations of the short-period structures were significantly less than the S_E DRS values of IBC 2015, as shown in Figure 7(d).

3.2. Response of Each Site Class. Figures 8–11 show the response spectra for each site class, S_B to S_E. The gray lines indicate the numerical analysis results of each site for the 18 earthquake accelerations. The blue line indicates the average of the analysis results. T_G indicates the period of the sites; T indicates the period of the structure models. The site period (T_G) was calculated from the first-mode frequency, f_1, of the wave-propagation transfer function. The reference EPGA for the 2,400-year return period was 0.22 g.

Figure 8 shows the results for four S_B sites. The periods of the soils (T_G) ranged from 0.048 to 0.075 s (Table 1). In the range of very short periods ($T < 0.2$ s), the maximum spectral accelerations of the numerical analyses were significantly greater than the IBC S_B design spectrum. The maximum response amplification occurred when the structure period (T) was the same as the site period (T_G). This result indicates that the response amplification was caused by resonance between the soil and the structure. However, in the ranges of structure periods (i.e., $T > 0.2$ s), the spectral accelerations were equivalent to the S_B design response spectrum of IBC 2015.

Figure 9 shows the results for four S_C sites. The average shear-wave velocities ($V_{S,30}$) of the four sites were similar (453, 454, 456, and 469 m/s, respectively), but the soil depth to bedrock values were significantly different (11.2, 26.0, 43.5, and 60.9 m, respectively). Thus, site periods were significantly different, $T_G = 0.13$, 0.22, 0.32, and 0.44 s, respectively, when the elastic soil property was assumed. Accordingly, the trend of the response amplification varied significantly. In the case of short site periods (where $T_G = 0.13$, 0.22, and 0.32 s in Figures 9(a)–9(c), respectively), the peak spectral accelerations were greater than the S_C DRS values of IBC 2015. However, the spectral accelerations for the longer periods ($T \geq 1.0$ s) were lower than the S_C DRS values of IBC 2015 and were close to the S_B DRS values of IBC 2015. For the longer site period of 0.44 s (Figure 9(d)), the spectral accelerations for the short periods (T) were equivalent to the S_C DRS values of IBC 2015, whereas the spectral accelerations for the long-period structures (T) were close to the S_B DRS values of IBC 2015.

Figure 10 shows the response spectra for four S_D sites. The spectral accelerations for the short site periods ($T_G = 0.25$ and

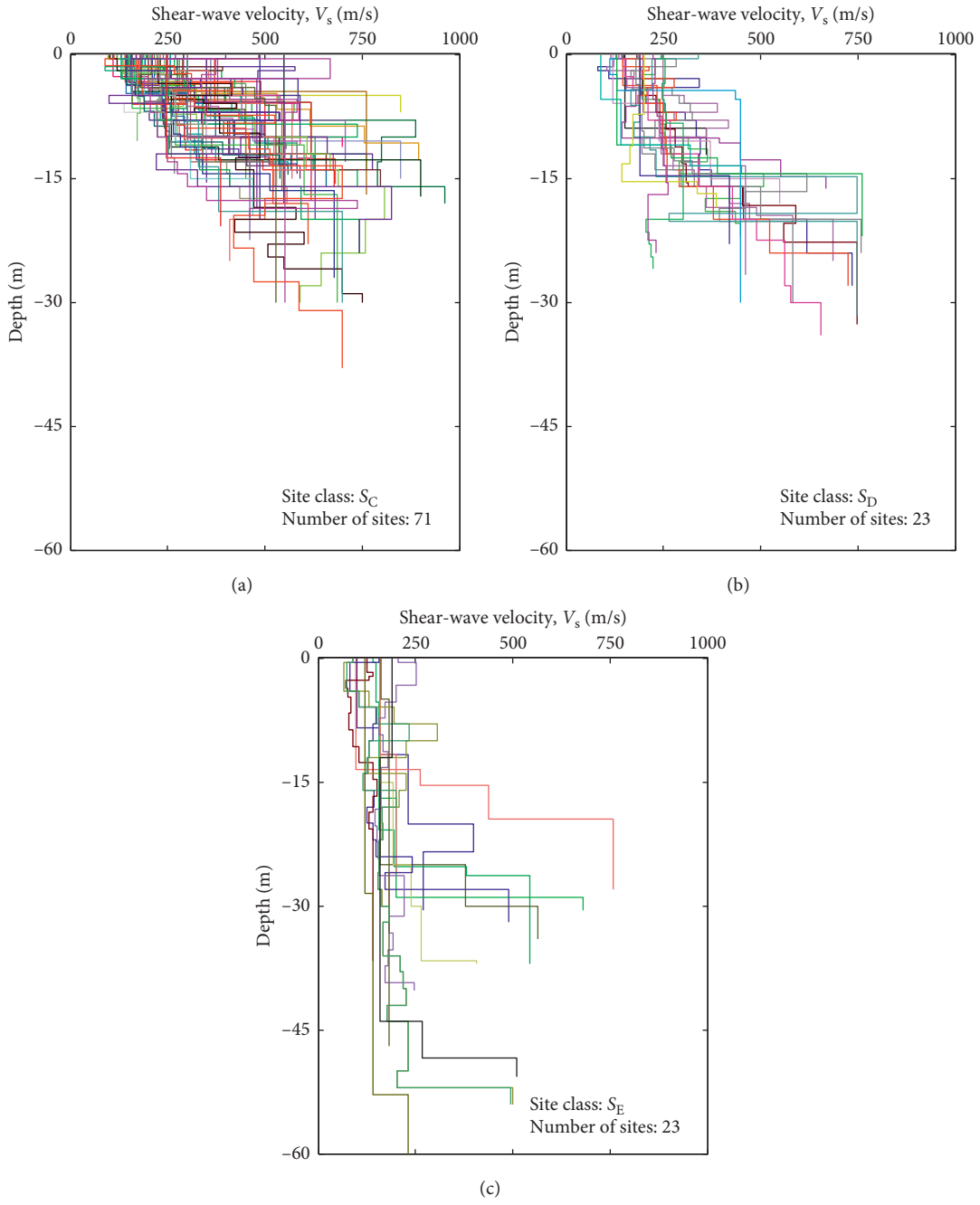

Figure 2: 109 shear-wave velocity profiles 378 soil strata from Lee et al. [11]. Site class: (a) S_C, (b) S_D, and (c) S_E.

Table 1: Summary of the soil properties of 487 sites.

Site class $V_{S,30}$	S_B			S_C			S_D			S_E		
Number of sites	9			302			161			15		
	Min	Max	Mean	Min	Max	Mean	Min	Max	Mean	Min	Max	Mean
Depth to bedrock (m)	6.03	10.1	7.06	5.3	91.6	28.7	12.2	84.1	46.1	28.0	54.0	40.6
$V_{S,30}$ (m/s)	765	835	793	360	754	480	238	359	339	114	179	160
Site period (s)	0.05	0.08	0.06	0.06	0.66	0.24	0.24	0.96	0.48	0.53	1.14	0.83

0.39 s in Figures 10(a) and 10(b), respectively) were close to the results of the S_C sites ($T_G = 0.22$ and 0.32 s in Figures 9(b) and 9(c), respectively). This result again confirms that the primary parameter for response amplification is the site period (T_G) rather than the material properties of the soil. Figures 10(c) and 10(d) shows the response spectra for the site

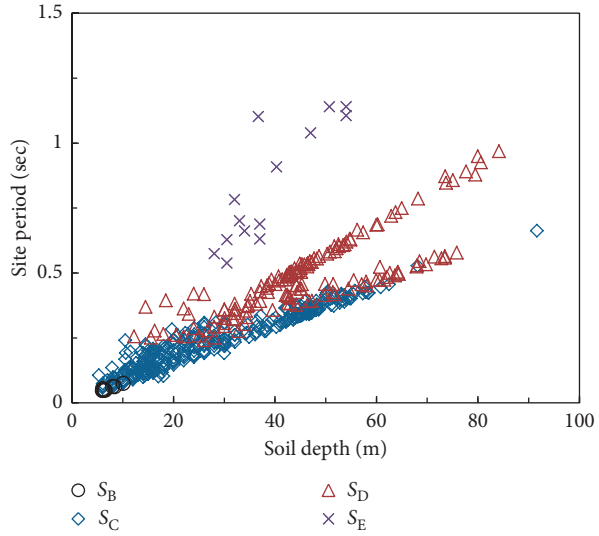

Figure 3: Site periods of 487 sites.

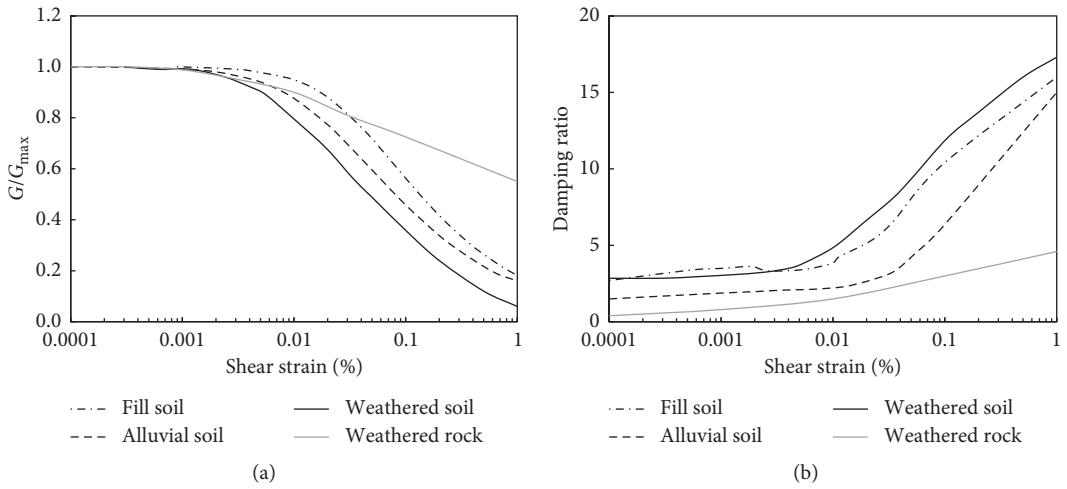

Figure 4: Nonlinear properties of the soil and rock. (a) Shear modulus. (b) Damping ratio.

Table 2: Properties of 12 recorded accelerations.

Event	Year	Nation	Station	Magnitude	Mechanism	R_{rup} (km)*
Irpinia-01	1980	Italy	Auletta	6.9	Normal	9.6
Denali	2002	USA	Carlo	7.9	Strike-slip	50.9
San Fernando	1971	USA	Cedar Springs	6.6	Reverse	89.7
Tabas	1978	Iran	Tabas	7.4	Reverse	2.0
Loma Prieta	1989	USA	So. San Francisco	6.9	Reverse	63.1
Chi-Chi	1999	Taiwan	HWA003	6.2	Reverse	50.4
Northridge-01	1994	USA	Vasquez Rocks Park	6.7	Reverse	23.6
Northridge-01	1994	USA	Antelope Buttes	6.7	Reverse	46.9
Duzce	1999	Turkey	Lamont 1060	7.1	Strike-slip	25.9
Irpinia-02	1980	Italy	Bagnoli Irpino	6.2	Normal	19.6
Kocaeli	1999	Turkey	Izmit	7.5	Strike-slip	7.2
Big Bear-01	1992	USA	Rancho Cucamonga	6.5	Strike-slip	59.4

*R_{rup}: closest distance to rupture plane.

periods $T_G = 0.79$ and 0.97 s, respectively. In the range of long-period structures ($T > 1.0$ s), the spectral accelerations were close to or less than the S_D DRS. However, for the short-period structures ($T < 1.0$ s), the spectral accelerations were close to or less than the S_B DRS, indicating that response amplification did not occur.

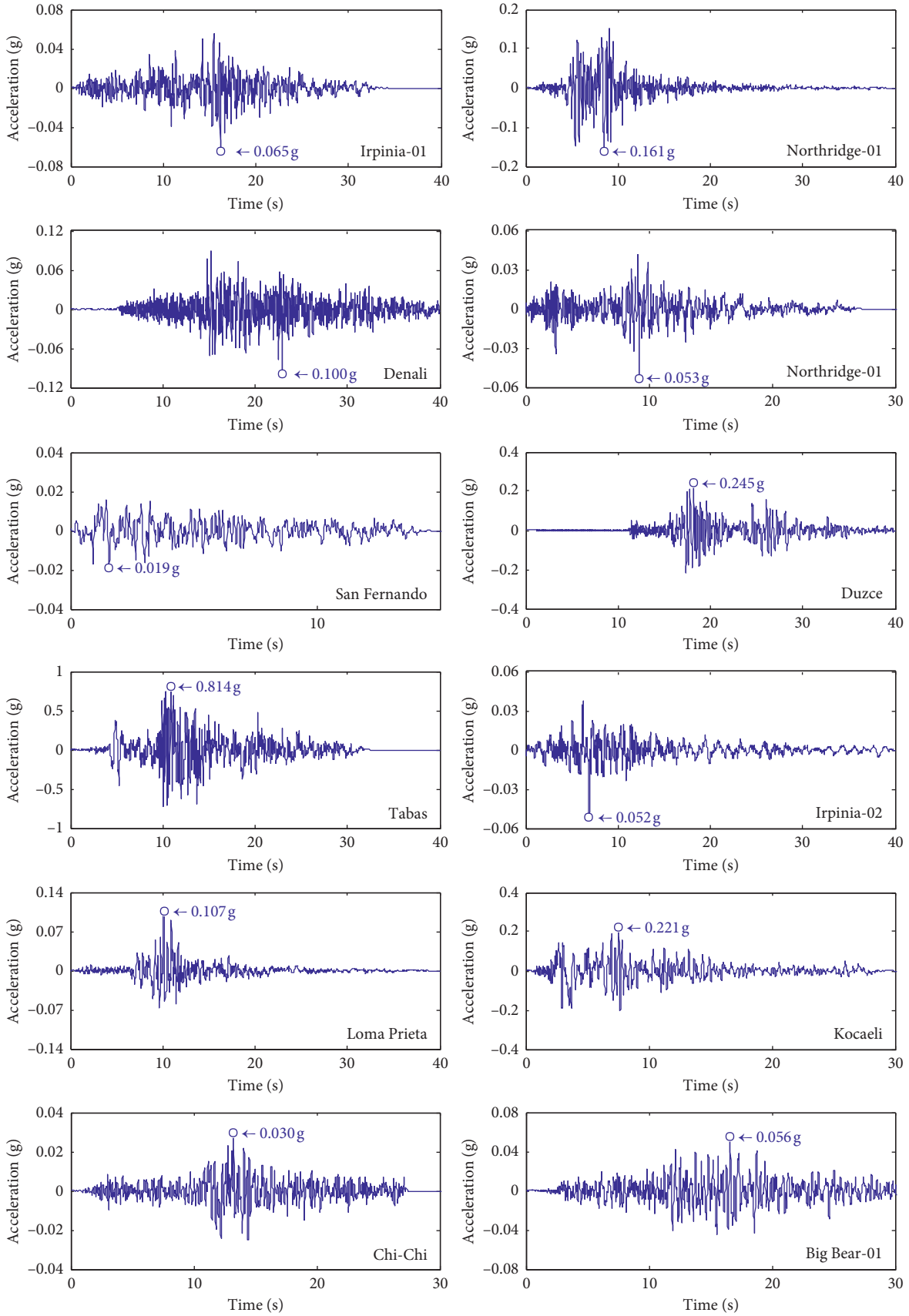

(a)

Figure 5: Continued.

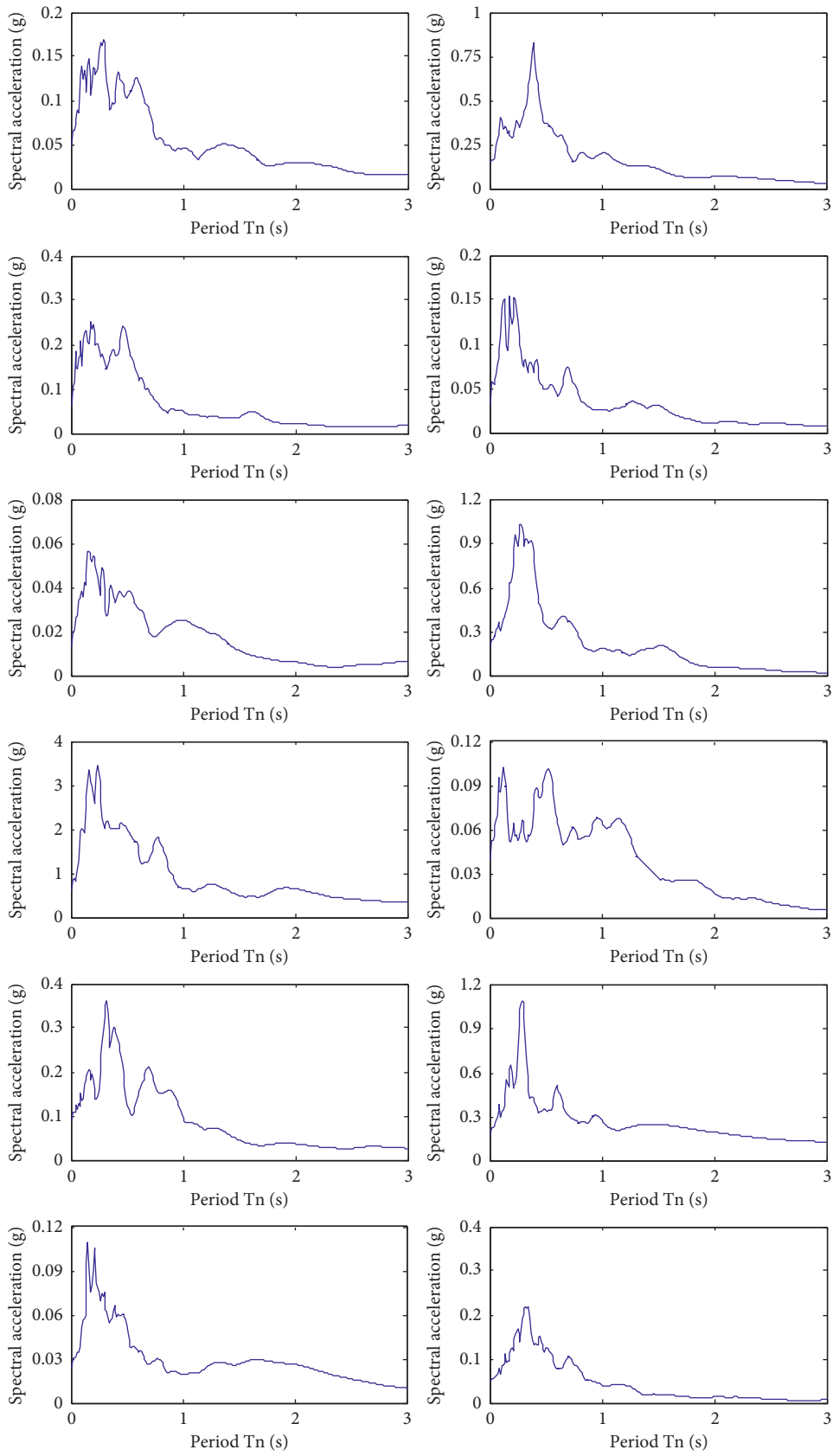

(b)

Figure 5: 12 actual and unscaled earthquake accelerations. (a) Acceleration time history. (b) Response spectrum.

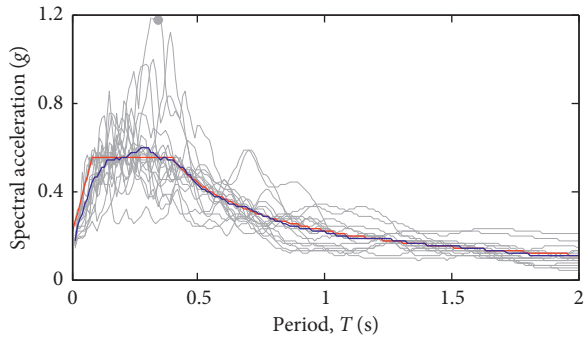

Figure 6: Average response spectra of input accelerations.

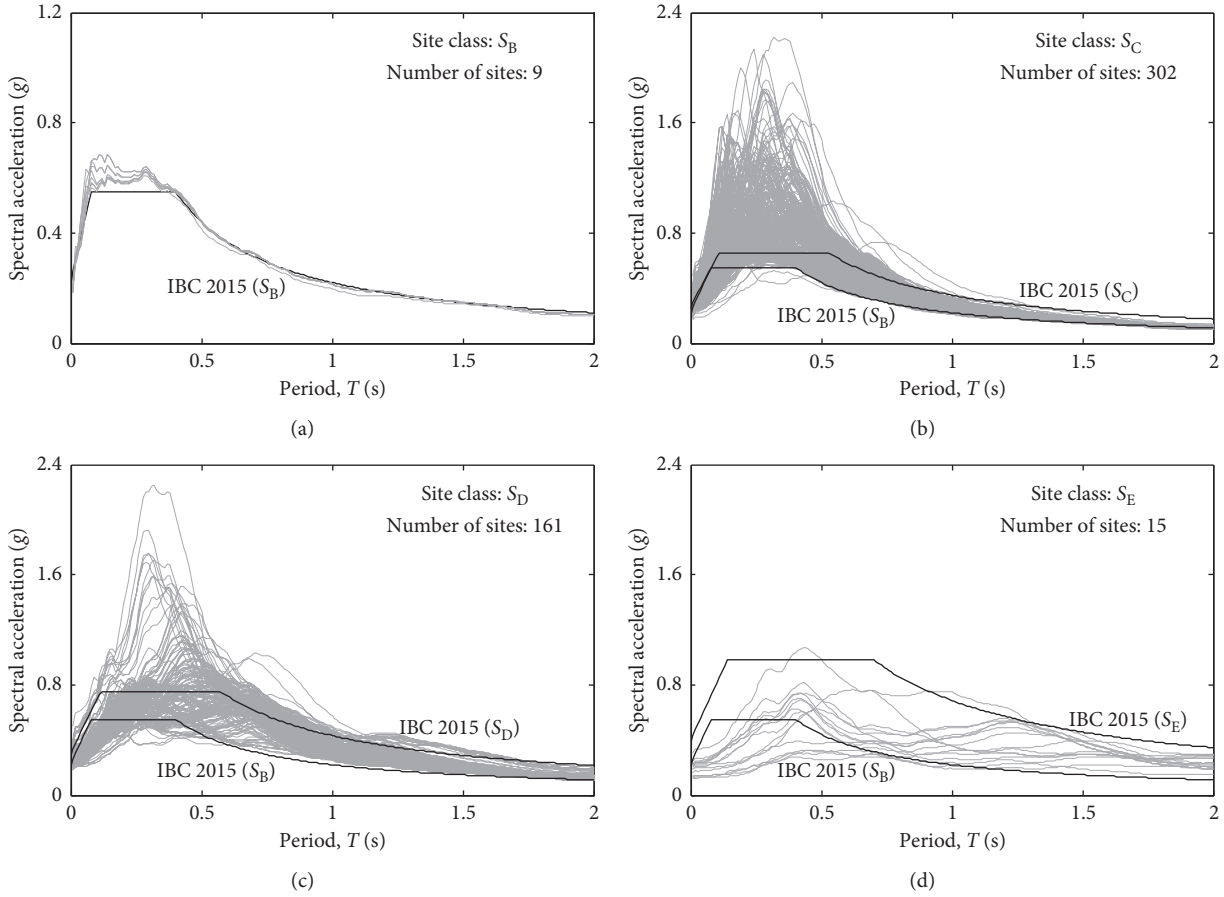

Figure 7: Response spectrum resulting from numerical analysis for 487 sites (reference effective peak ground acceleration (EPGA) = 0.22 g) for (a) S_B. (b) S_C. (c) S_D. (d) S_E.

Figure 11 shows the response spectra for four S_E sites. For the long-period structures, the spectral accelerations were close to the S_E DRS. For the short-period structures, the spectral accelerations were greater than the S_B DRS but were significantly less than the S_E DRS.

3.2.1. Step-1: Site Classification and Site Coefficients Based on $V_{S,30}$ (DRS-1). In IBC 2015, the DRS acceleration is defined as two-thirds of the maximum considered earthquake (MCE) spectral acceleration, with a return period of 2,400 years. The spectral accelerations are defined as follows [2]:

$$S_a = 0.6\frac{S_{DS}}{T_0}T + 0.4S_{DS}, \quad 0 \le T \le T_0, \tag{3}$$

$$S_a = S_{DS}, \quad T_0 \le T \le T_s, \tag{4}$$

$$S_a = \frac{S_{D1}}{T}, \quad T_s \le T, \tag{5}$$

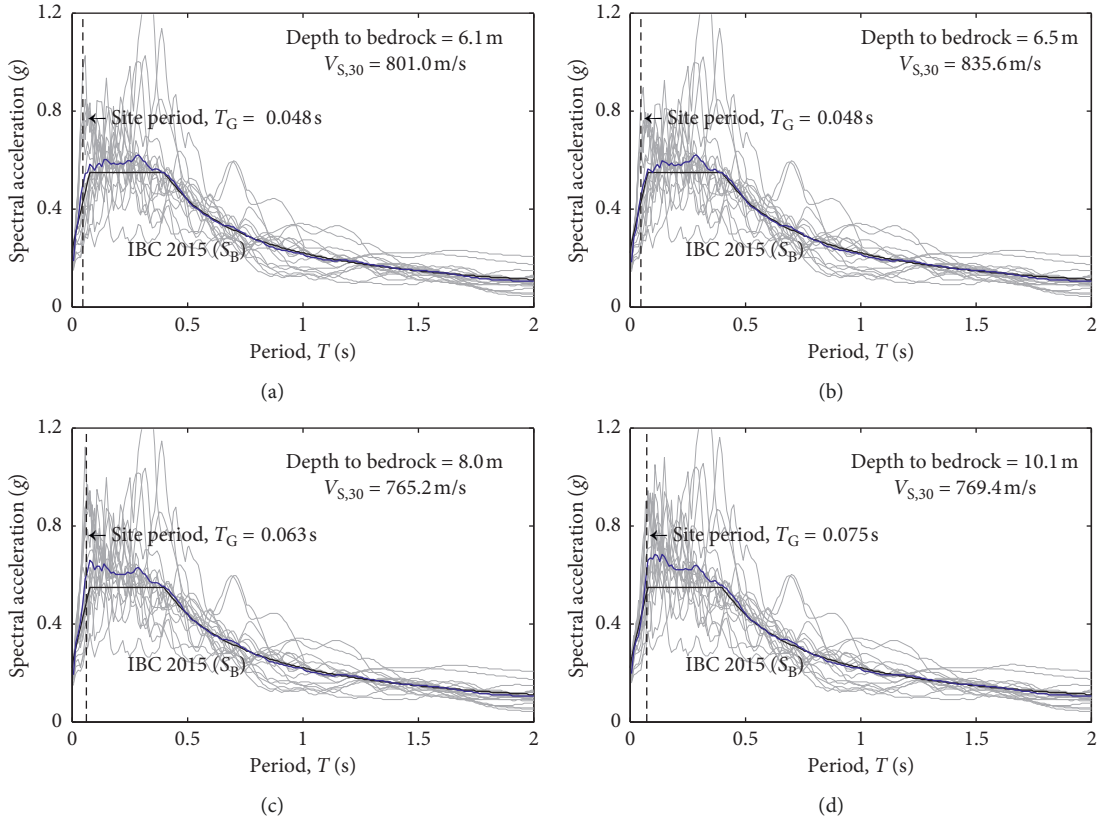

FIGURE 8: Response spectrum resulting from numerical analysis of four S_B sites with depth to bedrock: (a) 6.1 m. (b) 6.5 m. (c) 8.0 m. (d) 10.1 m.

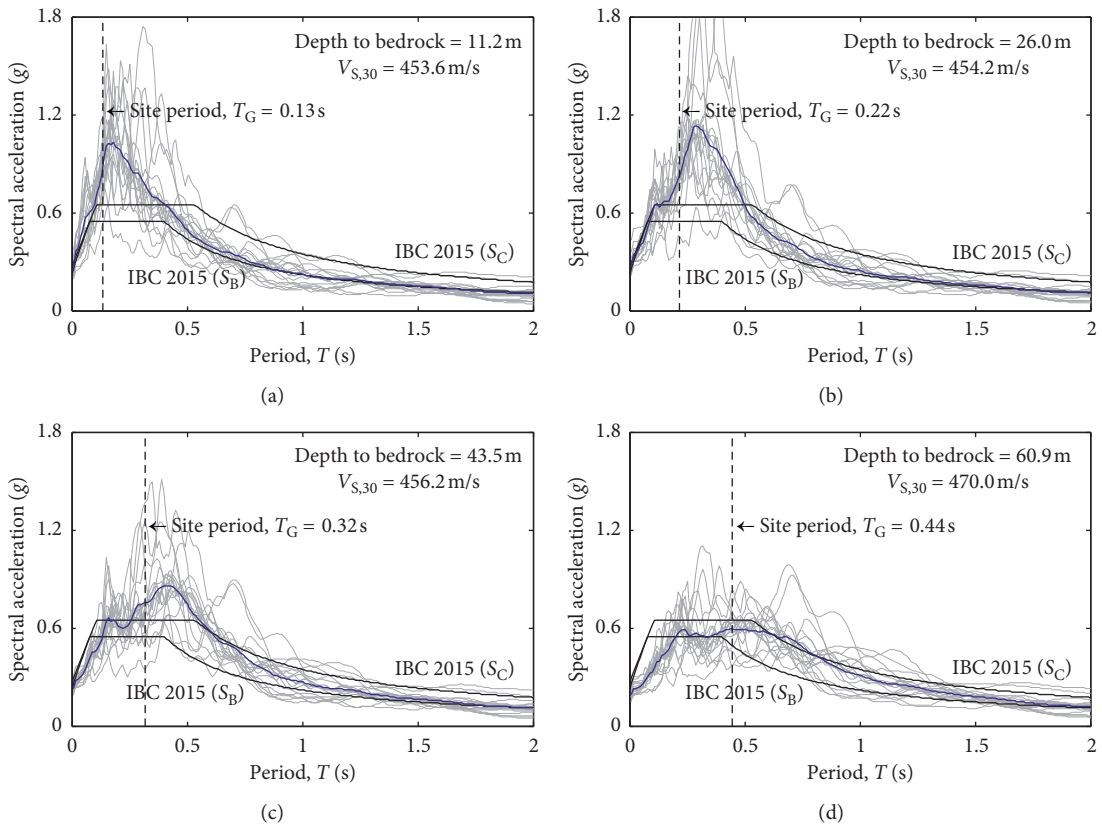

FIGURE 9: Response spectrum resulting from numerical analysis of four S_C sites with depth to bedrock: (a) 11.2 m. (b) 26.0 m. (c) 43.5 m. (d) 60.9 m.

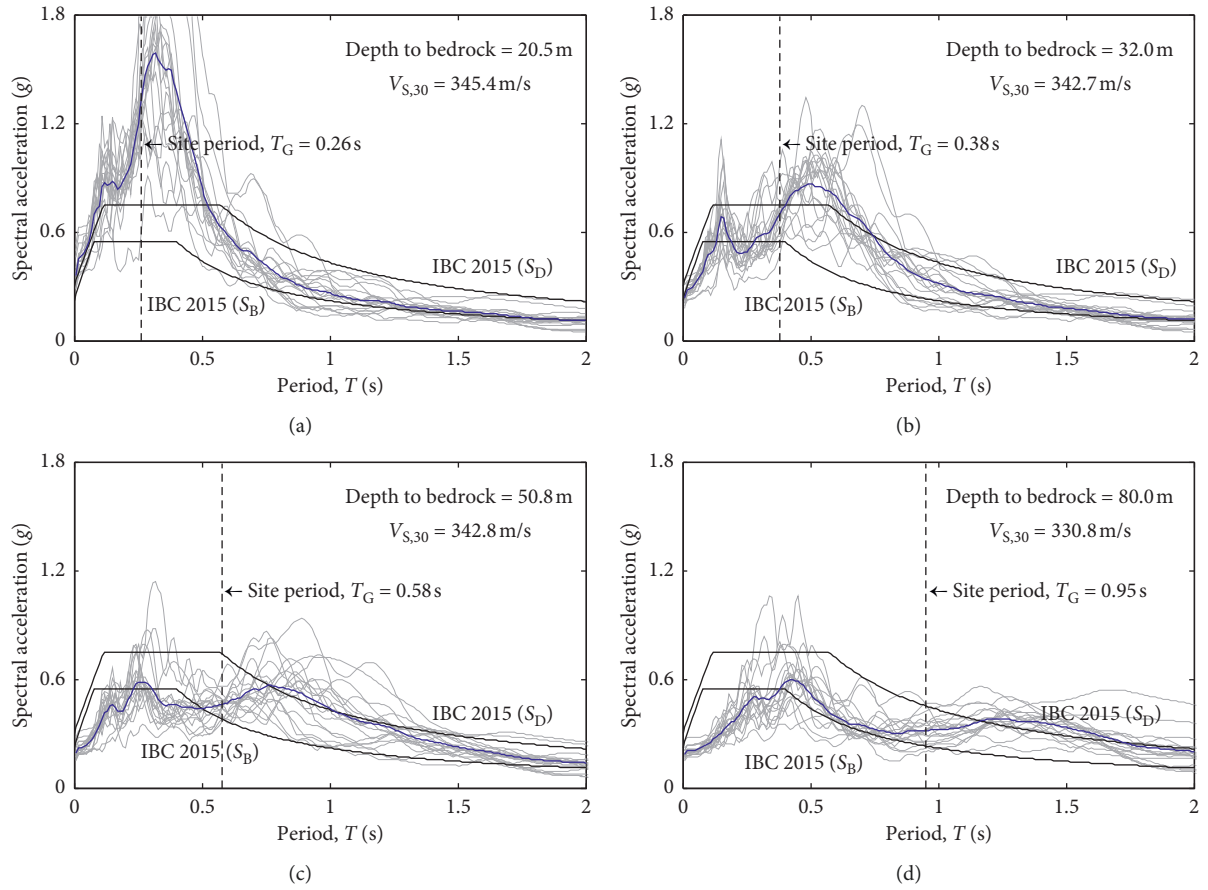

FIGURE 10: Response spectrum resulting from numerical analysis of four S_D sites with depth to bedrock: (a) 20.5 m. (b) 32.0 m. (c) 50.8 m. (d) 80.0 m.

where S_{DS} and S_{D1} are the design spectral accelerations for short periods and 1 s period, respectively. $S_{DS} = S \times 2.5 \times F_a \times (2/3)$, and $S_{D1} = S \times F_v \times (2/3)$. S is the reference effective ground acceleration for the rock site. $T_s = S_{D1}/S_{DS}$ and $T_0 = 0.2\,(S_{D1}/S_{DS})$. Equations (4) and (5) indicate the design spectral accelerations for the constant-acceleration range and the constant-velocity range, respectively.

To address the numerical analysis results in the DRS and soil factors, the short-period (constant acceleration-related) amplification factor F_a and the midperiod (constant velocity-related) amplification factor F_v were evaluated. The amplification factors were calculated as the ratio (RRS) of the response spectral value for the soil to the spectral value for the outcropping rock. According to FEMA 1997, F_a and F_v are defined as follows:

$$F_a\,(\mathrm{RRS}) = \frac{R_{soil}}{R_{rock}} \frac{1}{0.4} \int_{0.1}^{0.5} \frac{\mathrm{RS}_{soil}\,(T)}{\mathrm{RS}_{rock}\,(T)}\,dT, \tag{6}$$

$$F_v\,(\mathrm{RRS}) = \frac{R_{soil}}{R_{rock}} \frac{1}{1.6} \int_{0.4}^{2.0} \frac{\mathrm{RS}_{soil}\,(T)}{\mathrm{RS}_{rock}\,(T)}\,dT, \tag{7}$$

where $\mathrm{RS}_{soil}\,(T)$ and $\mathrm{RS}_{rock}\,(T)$ are the spectral accelerations corresponding to the soil and rock, respectively, at a given structure period T and R_{soil} and R_{rock} are the hypocentral distances from the soil and rock stations. The ratio R_{soil}/R_{rock} was assumed to be 1.0 in this study.

The calculated F_a and F_v are presented in Tables 3 and 4, according to the level of the EPGA. In the tables, "IBC 2015" refers to the amplification factors specified in IBC 2015 and "Analysis result" refers to the amplification factors (from equations (6) and (7)), based on the results of numerical analyses. The constant acceleration-related amplification factor F_a in IBC 2015 continues to increase as the site class changes from S_B to S_E. However, in the proposed DRS-1, the F_a value of S_C is greater than those of the S_D and S_E sites. For the S_E site, because the increased damping ratio due to the nonlinearity of soil reduced the site responses of higher orders, the mean value of F_a is less than 1.0.

In the case of the proposed F_v values, the response amplification increases as the site class changes from S_B to S_E. However, the amplification is less than that of IBC 2015. As the EPGA increases, the proposed F_v values decreases to close to those of IBC 2015, which is attributed to the decreased stiffness and increased damping of the nonlinear soil behavior.

Figure 12 compares the response spectra from (1) numerical analysis, (2) the proposed amplification factor (DRS-1), and (3) IBC 2015. The EPGA was 0.22 g. For the amplification factors of DRS-1, the mean (+) standard deviation

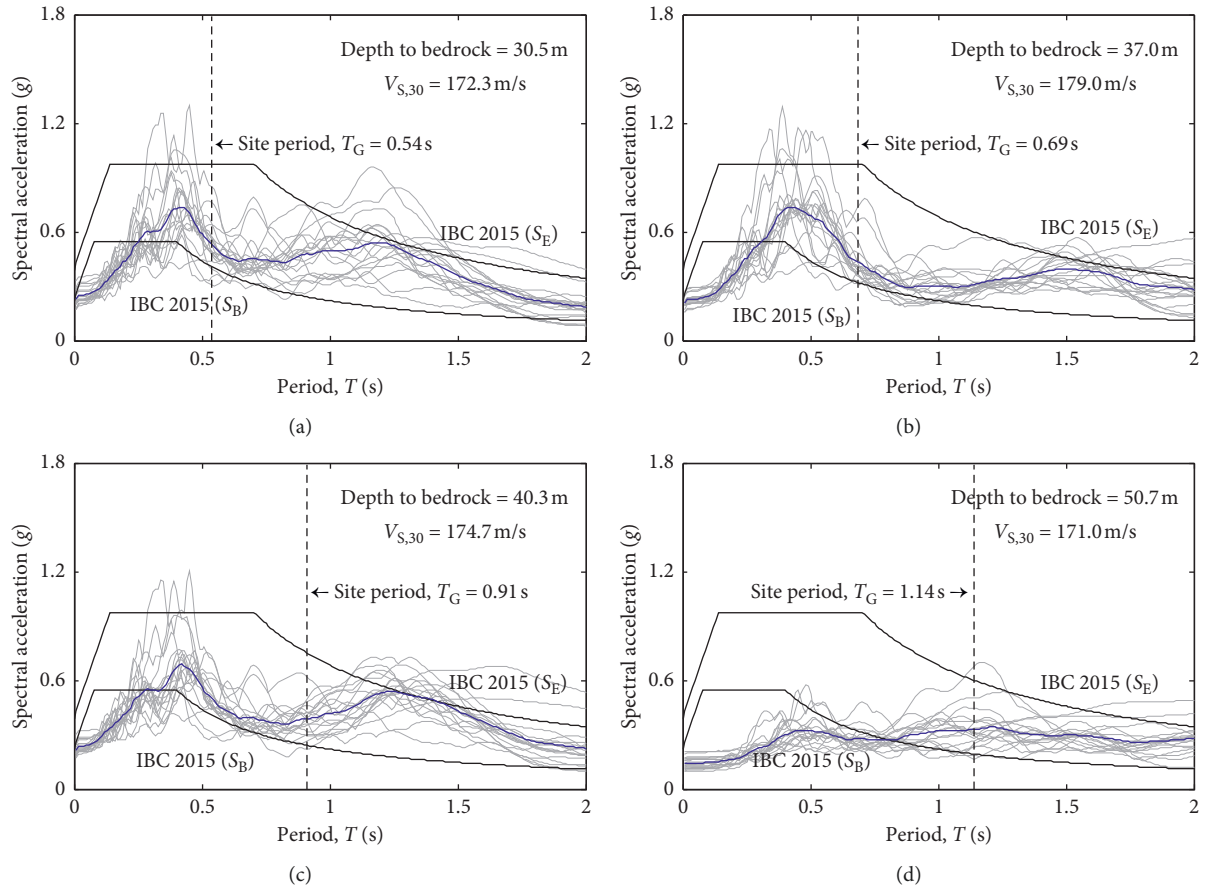

Figure 11: Response spectrum resulting from numerical analysis of four S_E sites with depth to bedrock: (a) 30.5 m. (b) 37.0 m. (c) 40.3 m. (d) 50.7 m.

Table 3: Short-period amplification factor (DRS-1).

	500-year return period (0.11 g)			1000-year return period (0.154 g)			2400-year return period (0.22 g)		
	IBC 2015	Analysis result		IBC 2015	Analysis result		IBC 2015	Analysis result	
		Mean	σ^*		Mean	σ		Mean	σ
S_B	1.00	1.06	0.019	1.00	1.06	0.019	1.00	1.06	0.024
S_C	1.20	1.58	0.296	1.20	1.55	0.307	1.18	1.51	0.320
S_D	1.58	1.50	0.328	1.49	1.42	0.337	1.36	1.27	0.359
S_E	2.44	1.06	0.336	2.18	0.98	0.338	1.78	0.82	0.316

*Standard deviation.

Table 4: Midperiod amplification factor (DRS-1).

	500-year return period (0.11 g)			1000-year return period (0.154 g)			2400-year return period (0.22 g)		
	IBC 2015	Analysis result		IBC 2015	Analysis result		IBC 2015	Analysis result	
		Mean	σ^*		Mean	σ		Mean	σ
S_B	1.00	1.00	0.001	1.00	1.01	0.001	1.00	1.00	0.021
S_C	1.69	1.15	0.123	1.65	1.17	0.130	1.58	1.21	0.148
S_D	2.36	1.49	0.141	2.18	1.51	0.141	1.96	1.56	0.126
S_E	3.47	2.01	0.265	3.34	1.97	0.300	3.12	1.85	0.384

in Tables 3 and 4 was used. Figure 12 shows the response spectra obtained from the numerical analysis results for the 487 sites in Korea. A response spectrum curve in the figure indicates the average of the response spectra for 18 input accelerations for a site condition. The numerical results were classified as S_B to S_E by the site class criterion, $V_{S,30}$. The number of sites that belonged to S_B, S_C, S_D, and S_E were 9, 302, 161, and 15, respectively.

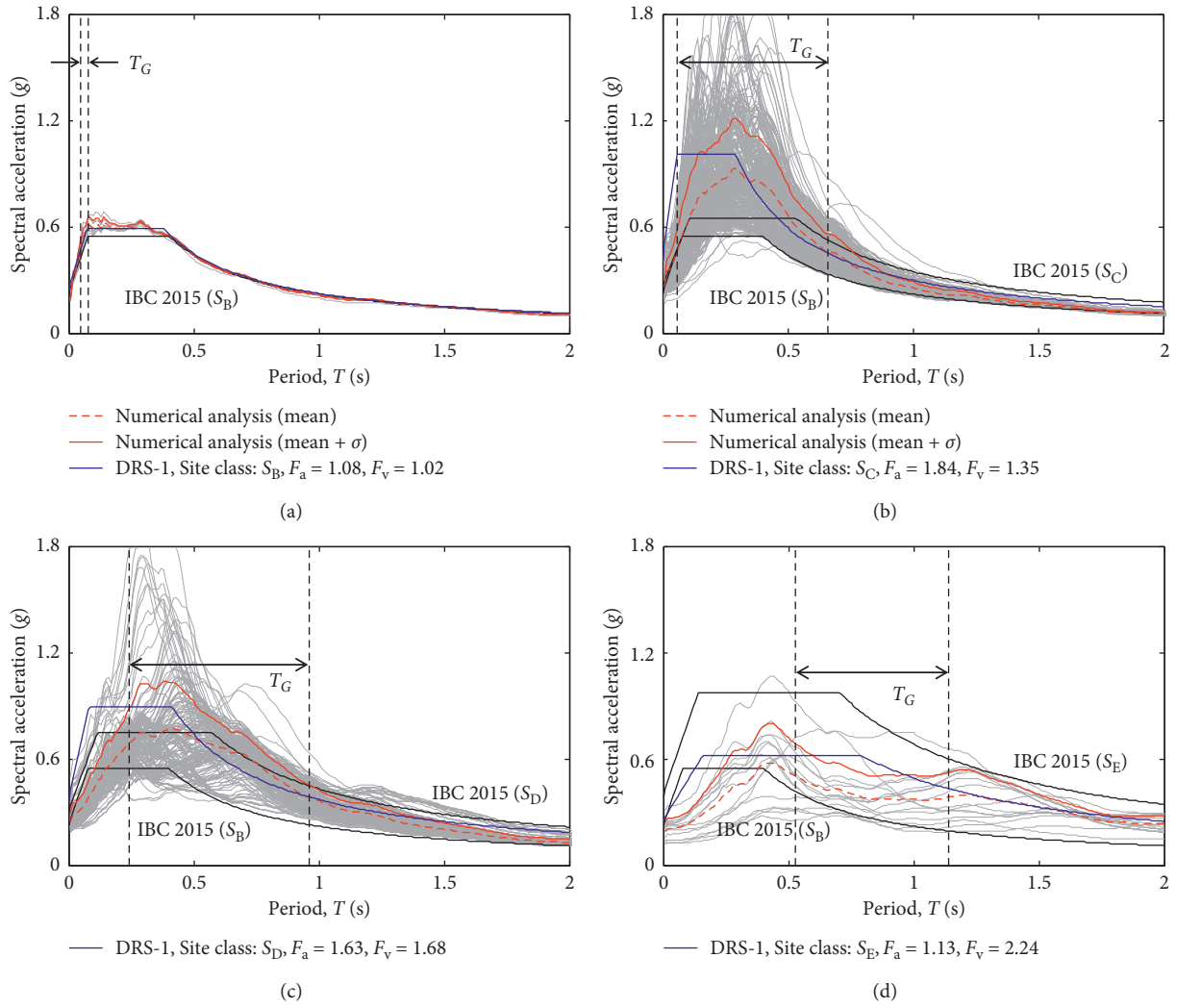

Figure 12: Comparison between numerical analysis results and DRS-1: (a) S_B. (b) S_C. (c) S_D. (d) S_E sites.

In Figure 12(a), for the S_B sites, the site coefficients F_a and F_v, estimated from numerical analysis, were close to 1.0 (Tables 3 and 4). The proposed response spectrum of DRS-1 is similar to the DRS in IBC 2015, except for the very short-period range. For the S_B sites in Korea (based on $V_{S,30}$), because the depth of the soil deposits was very shallow, ranging from 6.0 to 10.0 m, the dynamic period of the soil is very short. For this reason, in the numerical results, the structure responses in the range of very short periods were amplified significantly due to resonance between the soil and the structure. However, because F_a is defined in a relatively large range of short periods (0.1–0.5 s (equation (6))), the high response amplification for very short periods, less than 0.2 s, was not properly captured by the definition of F_a.

In the case of the S_C sites (Figure 12(b)), the proposed F_a value (mean + σ) is greater than that of the S_C class in IBC 2015, whereas the F_v value (mean + σ) is smaller. As the site periods of the S_C class range from 0.06 to 0.66 s, the maximum response amplification occurred in this range. This trend agrees with the results from previous studies ([9, 11]) for the shallow soil conditions in Korea. When the proposed site coefficients were used in the range of 0.2–0.7 s, the response spectral values of DRS-1 underestimated the maximum values obtained from the numerical analysis. In Figure 12(c), the trend of the DRS-1 for the S_D sites was similar to that for the S_C sites. The response spectral values of DRS-1 underestimated the maximum numerical results in the range of 0.3–0.8 s. For the S_E sites having $V_{S,30}$ values less than 180 m/s (Figure 12(d)), the proposed F_a value (mean + σ) was 1.13. In the short-period range, the DRS-1 was significantly less than the S_E DRS values in IBC 2015 and was close to the S_B DRS values. The proposed F_v value (mean + σ) was close to that of the S_D DRS values in IBC 2015. These results indicate that response amplification occurred only for the long-period structures and that the amplification was not significant.

In terms of the trends of the response amplification, design response spectra using the proposed site coefficients (DRS-1) differ from the analysis results. Particularly, for the S_C and S_D site classes, the DRS-1 does not accurately capture the maximum spectral accelerations and the amplification ranges affected by the site periods. These results indicate that

when the definitions for F_a and F_v coefficients of IBC are used, the DRS-1 can lead to unsafe seismic designs of structures.

As shown in Figures 8–11, although the site classes ($V_{S,30}$) are identical, the site periods can differ significantly, depending on the stiffness and depth of the soil deposits. For example, for the S_C site class ($V_{S,30}$), the site periods vary from 0.058 to 0.66 s in Table 1. Thus, it is unreasonable to define the dynamic properties of the soils with the $V_{S,30}$ values alone.

3.2.2. Step-2: Site Classification and Site Coefficients Based on Site Period (DRS-2). As mentioned in the previous section, site classification based on the $V_{S,30}$ does not accurately describe the characteristics of the site responses. Further, when the depth to bedrock is less than 30 m, the properties of the bedrock are included in the definition of $V_{S,30}$. However, when the depth to bedrock is greater than 30 m, the entire soil strata are not included in the site classification.

Thus, in DRS-2, the site period was used as the site class criterion, and the short-period and midperiod site amplification factors were defined according to the site period, as proposed in Figure 13. The amplification factors are summarized in Tables 5 and 6. The proposed amplification factors according to the site periods were calculated as follows:

$$F_a = \frac{1}{T_a - T_b} \int_{T_b}^{T_a} \frac{\mathrm{RS}_{soil}(T)}{\mathrm{RS}_{rock}(T)} dT, \tag{8a}$$

$$T_a = \min\left(1.3T_G, 0.65\right), \tag{8b}$$

$$T_b = \min\left(0.3T_G, 0.2\right), \tag{8c}$$

$$F_v = \frac{1}{0.5} \int_{1.0}^{1.5} \frac{\mathrm{RS}_{soil}(T)}{\mathrm{RS}_{rock}(T)} dT. \tag{9}$$

In equations (8a)–(8c), for F_a, the ranges T_a and T_b of the integration are defined by the site period T_G and the maximum period is limited to 0.65 s. For F_v, the range of the integration in equation (9) is reduced to safely define the amplification factors in the constant-velocity range.

In Figure 13(a), when the site periods are shorter than 0.3 s, the short-period amplification factors are greater than the amplification of 1.84 for the S_C site in Figure 12(b), calculated from equation (6). When the site period is outside the integration range, the amplification by the first mode of the soil deposits does not occur in the integration range. Thus, as the site periods increase beyond the integration range, the short-period amplification factors decrease gradually.

For the midperiod amplification factors, as the site periods increase, the amplification by the first mode of the soil deposits is included in the integration range. Thus, the midperiod amplification factors increase gradually.

When the sites are classified by the site period, Figure 14 shows the design response spectra (DRS-2) resulting from the site amplification factors, depending on the site period. The DRS-2 was compared with the numerical analysis results and the response spectra of the IBC 2015. The EPGA was 0.22 g.

In Figures 14(a)–14(d), when the site periods were in the range of 0.05–0.4 s, the short-period spectral accelerations of the DRS-2, calculated from equation (8a)–(8c), were close to the maximum spectral accelerations corresponding to the first-mode period of the soil deposits.

When the site periods range from 0.4 to 0.6 s (Figures 14(e) and 14(f)), the site period was increased by the nonlinear properties of the soil deposits and the amplification range was between the constant-acceleration range and the constant-velocity range. However, the midperiod amplification factor, F_v, was defined at the period of 1.0 s. Thus, in Figures 14(e) and 14(f), the midperiod site amplification factor of DRS-2 underestimates the response amplification by the intermediate site period.

Figures 14(g) and 14(h) show the DRS-2 of the sites with periods greater than 0.6 s. The responses of the long-period structures, affected by the first mode site periods, and the responses of the short period structures, affected by the higher modes of the soil deposits, are described well by the midperiod and the short-period site amplification factors.

As shown in Figures 14(b)–14(e), the response amplification occurred in the range of the site period. However, although the site amplification factors were defined with the site period, DRS-2 did not describe the response amplification. This is because the constant-acceleration range did not capture the range of the site amplification. This result indicates that when the site period is used for the site class criterion, the form of the design response spectrum as well as the site amplification factors should be defined by the site period.

3.2.3. Step-3: Proposed Design Response Spectrum-3 (DRS-3). The numerical analysis results showed that response amplification occurred due to resonance between the soil and structure and that the site periods varied with soil depth. To address these results, a new form of design response spectrum with three site classes is proposed.

First, the sites are classified into three site classes: (1) short-period sites ($T_G < 0.4$ s), (2) midperiod sites ($0.4 < T_G < 0.7$ s), and (3) long-period sites ($0.7\,\mathrm{s} < T_G$). On the basis of the amplification factors in Figure 13, amplification factors corresponding to the three site classes are proposed in Table 7. In the case of IBC 2015, the constant-acceleration range is determined by $T_s = (F_v/2.5\,F_a)$ and $T_0 = 0.2\,T_s$.

Figure 15 shows the proposed design response spectrum (DRS-3) that is defined by the site period, T_G. To include the first-mode periods of short-period sites or second-mode periods of midperiod and long-period sites, the constant-acceleration ranges are extended to T_1. T_2 is a corner period to include the response amplifications by the higher modes of soil deposits. To define the constant-velocity range, the spectral accelerations are moved horizontally by $(T_1 - T_s) : S_a = S_{D1}/(T - (T_1 - T_s))$ in Figure 15.

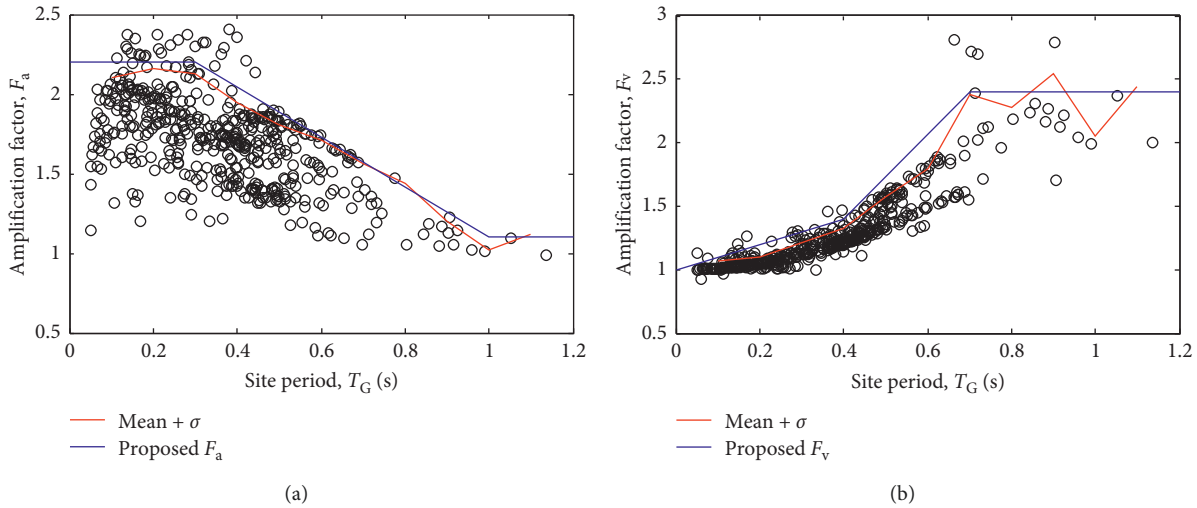

Figure 13: Site amplification factors according to site period (DRS-2): (a) F_a; (b) F_v.

In Figure 16, the proposed DRS-3 is compared with the numerical analysis results and the DRS of IBC 2015. DRS-3 agrees with the maximum accelerations and the constant-acceleration range calculated by the numerical analyses. Unlike DRS-1 and DRS-2, DRS-3 provides a better description of the range and magnitude of the maximum spectral values in the constant-acceleration range and less amplified spectral accelerations in the constant-velocity range.

4. Conclusions

Numerical studies were performed to investigate the response spectra for 487 site conditions in Korea, which is a moderate seismic zone with shallow soil depths. The magnitudes of the earthquake accelerations were scaled to the EPGAs of moderate seismic zones (0.11, 0.154, and 0.22 g). Twelve existing earthquake records and six artificial accelerations, which were adjusted to the target EPGAs, were used for the input ground accelerations. The numerical analysis results were compared with design response spectrum (DRS) values of IBC 2015. The results of the present study can be summarized as follows:

(1) Even within the same site class ($V_{S,30}$ in IBC 2015), the (elastic) periods of the sites varied significantly with soil depth.

(2) The spectral accelerations of structures were significantly amplified when the site period was close to the structure period. This result indicates that to accurately predict the effects of soil, the response-amplification factor (i.e., the soil factor) needs to be defined by the site period rather than by the soil shear modulus (or soil shear velocity).

(3) The responses of structures were amplified by the higher modes, as well as by the first mode of the soil deposit. The higher modes amplified the responses of short-period structures.

Table 5: Short-period amplification factor according to site period (DRS-2).

T_G (s)	0.0	0.3	$1.0 \le T_G$
F_a	2.2	2.2	1.1

Table 6: Midperiod amplification factor according to site period (DRS-2).

T_G (s)	0.0	0.4	$0.7 \le T_G$
F_v	1.0	1.4	2.4

(4) When the site periods were less than 0.4 s, the spectral accelerations were greater than the DRS values corresponding to the site class $V_{S,30}$ in IBC 2015. When the site periods ranged from 0.4 to 0.6 s, the spectral accelerations were close to the DRS values of IBC 2015. When the site periods were greater than 0.7 s, the spectral accelerations were less than the DRS values of IBC 2015.

(5) In particular, in the case of S_E soil ($V_{S,30} < 180$ m/s), the spectral accelerations were significantly less than the S_E DRS values and were close to the unamplified DRS values of S_B.

In this study, three steps for the design response spectrum (DRS) were performed to address the effect of shallow soil deposits (in Korea) on structure responses. In the first step, DRS-1, following the definitions of the site classification and the site coefficient of IBC 2015, the magnitude of the site coefficient was estimated based on the numerical analysis results. In the second step, DRS-2, the site period was used for the site classification and the integration ranges for the amplification factors were modified. In the third step, DRS-3, to enhance the accuracy of the DRS, both the magnitude and ranges of the response amplification were defined by the site period. Results of the three steps are summarized as follows:

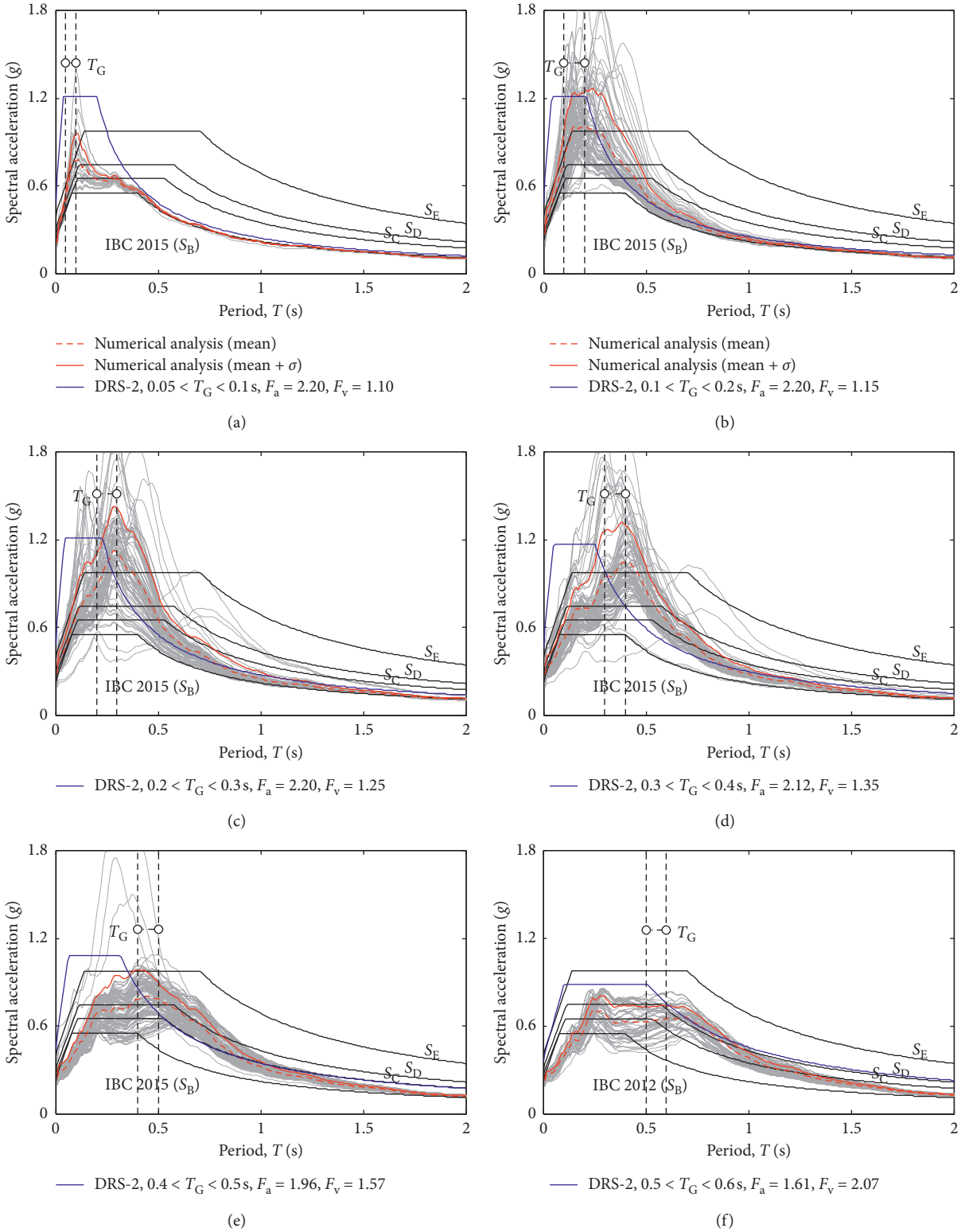

Figure 14: Continued.

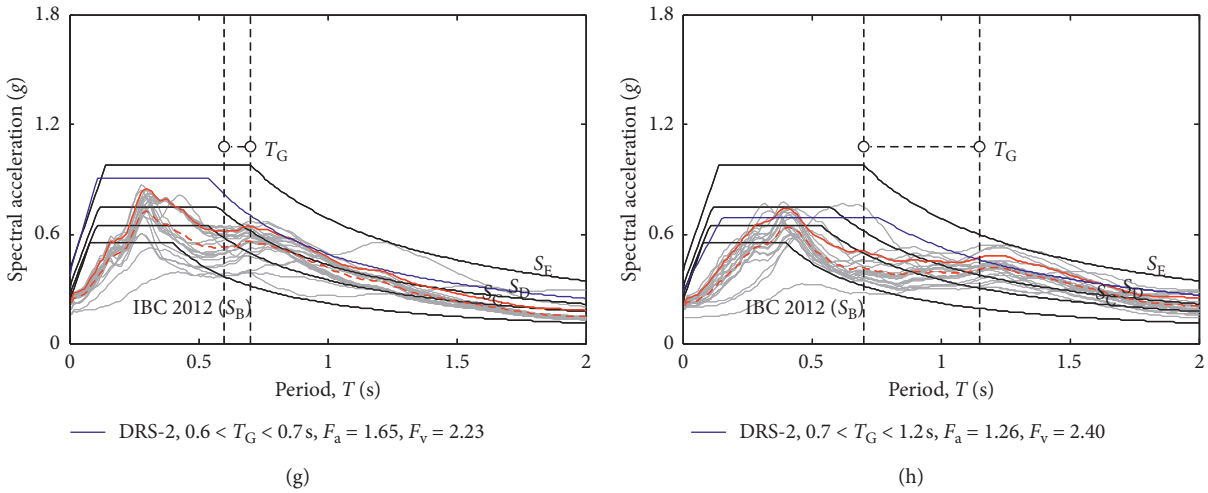

Figure 14: Comparison between numerical analysis results and DRS-2.

Table 7: Properties of the proposed DRS-3.

T_G	F_a	F_v	Constant-acceleration range			
			This study		IBC 2015	
			T_2	T_1	T_0	T_S
$T_G < 0.4$ s	2.2	1.4	0.1	0.4	0.056	0.28
0.4 s ≤ T_G < 0.7 s	1.7	1.6	0.2	0.6	0.08	0.38
0.7 s ≤ T_G	1.4	2.4	0.3	0.9	0.14	0.69

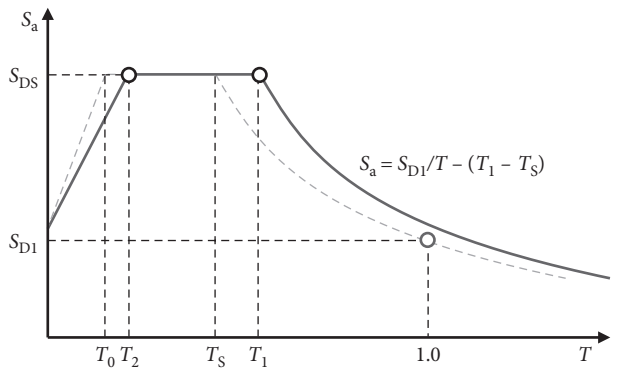

Figure 15: New form of design response spectrum (DRS-3).

(1) The DRS of the IBC was developed with the analysis of seismic ground motions measured at sites located on the West Coast of the United States that have deep soil deposits. However, in this study, DRS-1 underestimated the short-period spectral accelerations resulting from numerical studies, with a large deviation. This indicates that the site classification based on $V_{S,30}$ and the constant-acceleration range did not rationally describe the responses of structures affected by shallow soil depth.

(2) In DRS-2, the constant-acceleration range of the short period sites did not accurately predict the range of the maximum responses resulting from the numerical analysis results. Thus, DRS-2 showed unsafe values for sites with periods of 0.1–0.5 s.

(3) DRS-3 generally agreed with the numerical results and described the characteristics of the response spectrum affected by shallow soil deposits well. For short site periods, the constant-acceleration range was narrow and the magnitude was greater than that of IBC 2015. As the site period increased, the range of

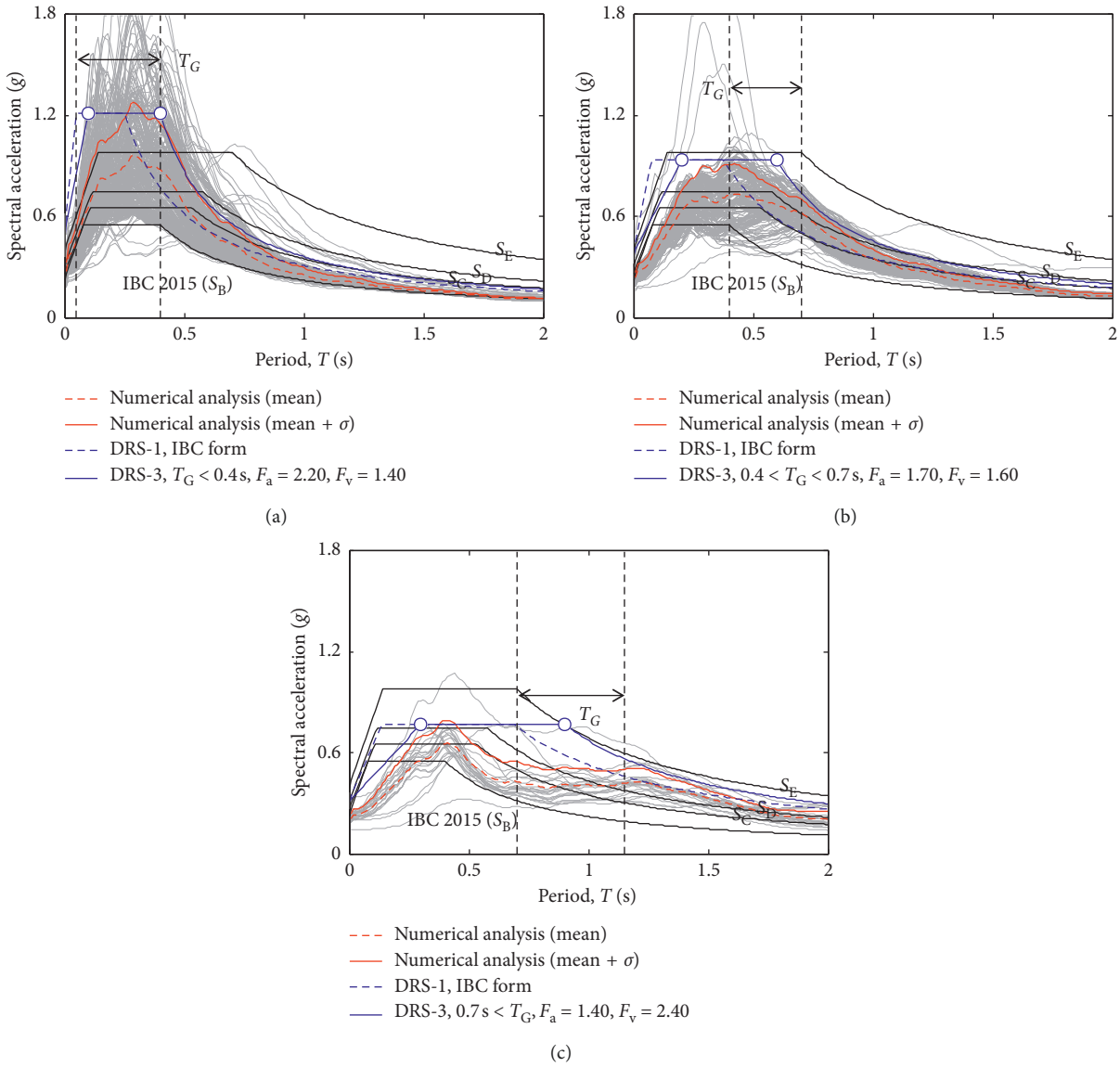

Figure 16: Comparison between numerical analysis results and DRS-3: (a) short-period sites. (b) Midperiod sites. (c) Long-period sites.

the constant acceleration increased, being shifted to greater periods, and the peak acceleration decreased.

Data Availability

The Excel file data used to support the findings of this study are available from the corresponding author upon request.

Conflicts of Interest

The authors declare that they have no conflicts of interest.

Acknowledgments

This research was supported by the Korea Agency for Infrastructure Technology Advancement (KAIA) funded by the Ministry of Land, Infrastructure and Transport (No. 18AUDP-B106327-04) and the Basic Science Research Program through the National Research Foundation of Korea (NRF) funded by the Ministry of Education(NRF-2018R1A6A1A07025819).

References

[1] Architectural Institute of Korea (AIK), *Korean Building Code*, Architectural Institute of Korea (AIK), Seoul, Republic of Korea, 2016.

[2] International Code Council (ICC), *International Building Code*, International Code Council (ICC), 2015.

[3] Federal Emergency Management Agency (FEMA), "NEHRP recommended provisions for seismic regulations for new buildings and other structures," Report No. FEMA-302, Building Seismic Safety Council, Washington, DC, USA, 1997.

[4] GB50011-2001, *Code for Seismic Design of Buildings*, China Building Industry Press, Beijing, China, 2001.

[5] A. Tena-Colunga, U. Mena-Hernández, L. Pérez-Rocha, J. Avilés, M. Ordaz, and J. Vilar, "Updated seismic design guidelines for model building code of Mexico," *Earthquake Spectra*, vol. 25, no. 4, pp. 869–898, 2009.

[6] European Committee for Standardization, *Eurocode 8: Design of Structures for Earthquake Resistance*, British Standard, London, UK, 2003.
[7] Mid-America Earthquake Center (MAE Center), "Uniform hazard ground motion and response spectra for mid-America cities," MAE Center Report 03-07, Mid-America Earthquake Center (MAE Center), Urbana, IL, USA, 2003.
[8] H. H. M. Hwang, H. Lin, and J.-R. Huo, "Site coefficients for design of buildings in eastern United States," *Soil Dynamics and Earthquake Engineering*, vol. 16, no. 1, pp. 29–40, 1997.
[9] D.-S. Kim and J.-K. Yoon, "Development of new site classification system for the regions of shallow bedrock in Korea," *Journal of Earthquake Engineering*, vol. 10, no. 3, pp. 331–358, 2006.
[10] C.-G. Sun, H.-S. Kim, C.-K. Chung, and H.-C. Chi, "Spatial zonations for regional assessment of seismic site effects in the Seoul metropolitan area," *Soil Dynamics and Earthquake Engineering*, vol. 56, pp. 44–56, 2014.
[11] S.-H. Lee, C.-G. Sun, J.-K. Yoon, and D.-S. Kim, "Development and verification of a new site classification system and site coefficients for regions of shallow bedrock in Korea," *Journal of Earthquake Engineering*, vol. 16, no. 6, pp. 795–819, 2012.
[12] D. S. Kim and Y. W. Choo, "Dynamic deformation characteristics of cohesionless soils in Korea using resonant column tests," *Journal of the Korean Geotechnical Society*, vol. 17, no. 5, pp. 115–138, 2001.
[13] I. M. Idriss and J. I. Sun, *A Computer Program for Conducting Equivalent Linear Seismic Response Analysis of Horizontally Layered Soil Deposits*, Civil Engineering Department, Center for Geotechnical Modelling, U.C. Davis, Davis, CA, USA, 1992.
[14] http://ngawest2.berkeley.edu/.
[15] S. A. Nikolaou, *A GIS Platform for Earthquake Risk Analysis*, Ph.D. dissertation, State University of New York, Buffalo, NY, USA, 1998.
[16] F. Naeim, A. Alimoradi, and S. Pezeshk, "Selection and scaling of ground motion time histories for structural design using genetic algorithms," *Earthquake Spectra*, vol. 20, no. 2, pp. 413–426, 2004.
[17] D. A. Gasparini and E. H. Vanmarche, *Simulated Earthquake Motions Compatible with Prescribed Response Spectra*, Report No. R76-4, MIT Department of Civil Engineering, Cambridge, MA, USA, 1976.
[18] American Society of Civil Engineers Standard (ASCE), *Seismic Analysis of Safety-Related Nuclear Structures and Commentary*, ASCE 4-98, Reston, VA, USA, 2000.
[19] Ministry of Construction and Transportation (MCT), *Seismic Design Standard Research*, Ministry of Construction and Transportation (MCT), Seoul, Korea, 1997.